Research Article | Vol. 30, No. 13 / 20 Jun 2022 / Optics Express 23090
Optics EXPRESS

Investigation of high-harmonic cutoff of metal ions driven by near-infrared laser

WUFENG FU,[1,2] YU HANG LAI,[3,*] JINGGUANG LIANG,[1,2] AND WEI LI[1,2,4]

[1]GPL, State Key Laboratory of Applied Optics, Changchun Institute of Optics, Fine Mechanics and Physics, Chinese Academy of Sciences, Changchun 130033, China
[2]University of Chinese Academy of Sciences, Beijing 100049, China
[3]Department of Physics, The Chinese University of Hong Kong, Hong Kong SAR, China
[4]weili1@ciomp.ac.cn
[*]yuhanglai@cuhk.edu.hk

Abstract: The cutoff-energies of high-harmonic generation in the laser-ablated plumes of various metal targets (Ca, Mg, Fe, Zn, Ta, Mo, Al, W, In, Cu, Au, Ti, Ag) driven by near-infrared (0.8-μm) femtosecond laser are investigated and compared. Due to the low ionization potentials of metal atoms, it is believed that the observed high-harmonic cutoffs are contributed by the singly charged or even doubly charged ions. Ionization calculations using Perelomov-Popov-Terent'ev theory are performed to estimate the laser intensities at which saturation of ionization occur for different ions. Treating the calculated values as the effective driving laser intensities, the observed cutoffs from most of the targets are in reasonable agreement with the predictions of the semi-classical cutoff law.

1. Introduction

High-harmonic generation (HHG) is a major research topic in strong-field atomic physics. It is an effective way to generate ultrashort extreme ultraviolet pulses and has become a useful tool for studying ultrafast dynamics [1,2] over the last two decades. While gaseous atoms have been the most routinely used generation media, low-density plasma plumes produced by laser ablation from solid surfaces have been recognized as an interesting alternative type of medium [3–5]. Due to the low densities of the plasmas, the fundamental HHG process is considered to be originated from the independent response of the individual atoms/ions in the plasma plume, similar to HHG in gaseous atoms. Employing the method of laser-ablated plasma plumes (LPPs) could drastically widen the choices of atom species for HHG since the method could be applied to virtually any material surfaces. Numerous interesting phenomena have been discovered. For instance, the harmonic spectra from the LPPs of several different metals exhibit drastic narrowband resonant enhancement [5–9] at some specific harmonic orders due to the special electronic structures of these metal ions [10–13].

At the single-atom level, HHG is well described by the Lewenstein's model [14], from which the cutoff law for the harmonic energy is $E_{cutoff} = 3.17U_P + I_P$, where U_P and I_P are the ponderomotive energy of the freed electron and the ionization potential of the atom, respectively. Experiments of HHG in gases have shown that the measured cutoff values are in reasonable agreement with this cutoff law [15,16], it was clearly observed that the cutoff depends on the I_p of the target atoms [17–19]. As for the studies of HHG from LPPs, the cutoffs of the harmonic spectra from a variety of targets have been reported in different papers [6,20–27]. However, in many cases the observed differences between different targets do not seem to agree well with the cutoff law if one simply considers the difference in I_P of the atomic form of the target. One of the complications in HHG in LPPs is the fact the plasmas do not only contain atoms but also ions of different charge states. It is very difficult, if not impossible, to accurately measure the

#455265 https://doi.org/10.1364/OE.455265
Journal © 2022 Received 1 Feb 2022; revised 28 Apr 2022; accepted 11 May 2022; published 9 Jun 2022

Optics EXPRESS

relative abundances of different ions in the LPPs, and the contributions of different ions to the measured harmonic spectra could not be separated. Although it is reasonable to anticipate that contributions of the ions could be the origin of the seemingly discrepancy between the measured and the predicted cutoffs, there is still a lack of systematic studies focused on addressing this issue.

In this work, we perform a comparative study on the harmonic cutoffs of LPPs of different metals (Ca, Mg, Fe, Zn, Ta, Mo, Al, W, In, Cu, Au, Ti, Ag) at the driving wavelength of 0.8 μm with the intensity range of 300–500 TW/cm^2. The lowest and the highest observed cutoffs are the 15th harmonic order (from Ca) and the 59th harmonic order (from Ag), respectively. Using the Perelomov-Popov-Terent'ev (PPT) theory for strong-field ionization [28], we calculate the saturation intensity I_{sat} (i.e., the laser intensity at which the ionization probability approaches one) for the atoms and ions of the used metals. In essence, I_{sat} roughly represents the maximum effective laser intensity for driving the HHG process in the target atom/ion. Since the I_P of the neutral atoms for all the metals we considered are very low, the values of I_{sat} are well below 100 TW/cm^2, which implies that the measured harmonic cutoffs are much higher than the theoretical cutoffs using the calculated I_{sat} values. However, if the theoretical cutoffs are calculated using the I_{sat} of singly charged ions (~100 TW/cm^2) or even doubly charged ions, reasonable agreement with the experiments are achieved for the majority of the considered cases.

2. Experimental setup

In this experiment, a commercial 1kHz, 0.8-μm Ti:sapphire amplifier system (Spectra Physics: Sprifire Ace) is used. A small portion of the energy of the amplified laser beam in the system is split into two beams before temporal compression. One of them is sent out without compression (210ps, 0.5mJ), which interacts with the sample surface as heating pulse (HP) to generate plasma plume by ablation. The other beam is compressed (35fs, 5.5mJ), which can be used as a driving pulse (DP) to interact with the plasma plume ablated from the target to generate high-order harmonics. Due to propagation through transmissive optical components and optical path in air, the 35-fs DP is broadened to about 52 fs when it arrives at the experimental setup. HP is focused on the sample surface through a 200 mm lens. The full width at half maximum (FWHM) of the focal spot is about 70μm. After the plasma plume is ablated by HP with a delay of about 50 ns, DP is focused into the plasma plume through a spherical lens with a focal length of 500mm. The FWHM of the focusing spot is about 90μm. The harmonics radiation which generated by DP interacting with plasma plume enters a home-built extreme ultraviolet spectrometer. After passing through a narrow slit, the harmonics radiation is first reflected by a concave mirror onto a 1200 grooves/mm flat field grating, then the dispersed harmonics are detected by a microchannel plate with a phosphor screen and accepted by a CCD camera. The spectrometer is calibrated by the known wavelengths of the emission lines of the generation medium. The acquisition time for each harmonic spectrum is set to be 200 ms. A schematic diagram of the experimental setup is shown in Fig. 1.

Optics EXPRESS

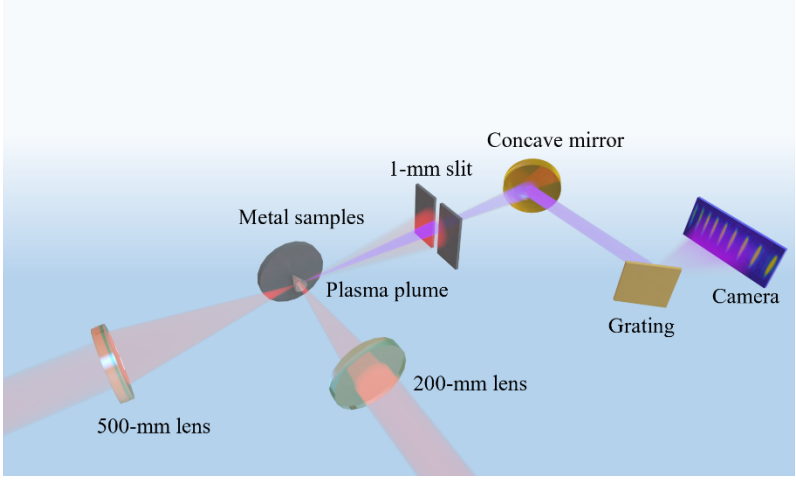

Fig. 1. Schematic diagram of the experimental setup.

3. Results and discussion

The types of metal elements used in this work are shown in Table 1. The values of I_P for the neutral atom, singly charged ion, and doubly charged ions of each species are also summarized. For the experiments on each element, the harmonic cutoff is optimized by fine adjusting the lateral distance between the DP beam and the sample surface and the distance between the plasma and the DP focus. The harmonic spectra are measured as a function of DP and HP intensities with the aim of observing the maximum attainable harmonic cutoff. At a fixed DP, the overall harmonic yield increases with HP intensity, which is mostly like just due to the fact that particle density increases with HP. Nevertheless, it should not lead to an increase in the harmonic cutoff energy. Note that it is not preferred to use a too intense HP because plasma emssions may become noticeable in the measured harmonic spectrum. For all spectra presented below, the HP intensity is fixed at about 10 GW/cm^2. It is found that such level of HP intensity is sufficient to gives satisfactory harmonic yields without noticeable plasma emissions.

Table 1. Ionization energies of metal atoms and ions.

Metal	I_p I (eV)	I_p II (eV)	I_p III (eV)
Ca	6.11	11.87	50.91
Mg	7.65	15.04	80.14
Fe	7.90	16.20	30.65
Zn	9.39	17.96	39.72
Ta	7.55	16.20	23.10
Mo	7.09	16.16	27.13
Al	5.99	18.83	28.45
W	7.86	16.37	26.00
In	5.79	18.87	28.04
Cu	7.73	20.29	36.84
Au	9.23	20.20	30.00
Ti	6.83	13.58	27.49
Ag	7.58	21.48	34.80

Optics EXPRESS

For most of the targets, it is typically found that the harmonic cutoff does not further increase noticeably as the DP reaches the range between 300 TW/cm^2 and 500 TW/cm^2. The comparisons throughout the following discussions are based on the maximum attainable harmonic cutoff of each element in our experiments.

Consistent with previous studies in the literature [29], it is found that the harmonic cutoff varies significantly between different targets. Figure 2 displays the harmonic spectra from all the targets listed in Table 1. The results are arranged in ascending order by harmonic cutoff. Ca and Mg, whose cutoffs are the 15th and 25th order, are the lowest among all the targets. On the other hand, the harmonic cutoff of Ag (59th order) and Ti (57th order), as shown in Fig. 2(d), are two of the highest. Figure 3 summarizes the harmonic cutoff from all the targets.

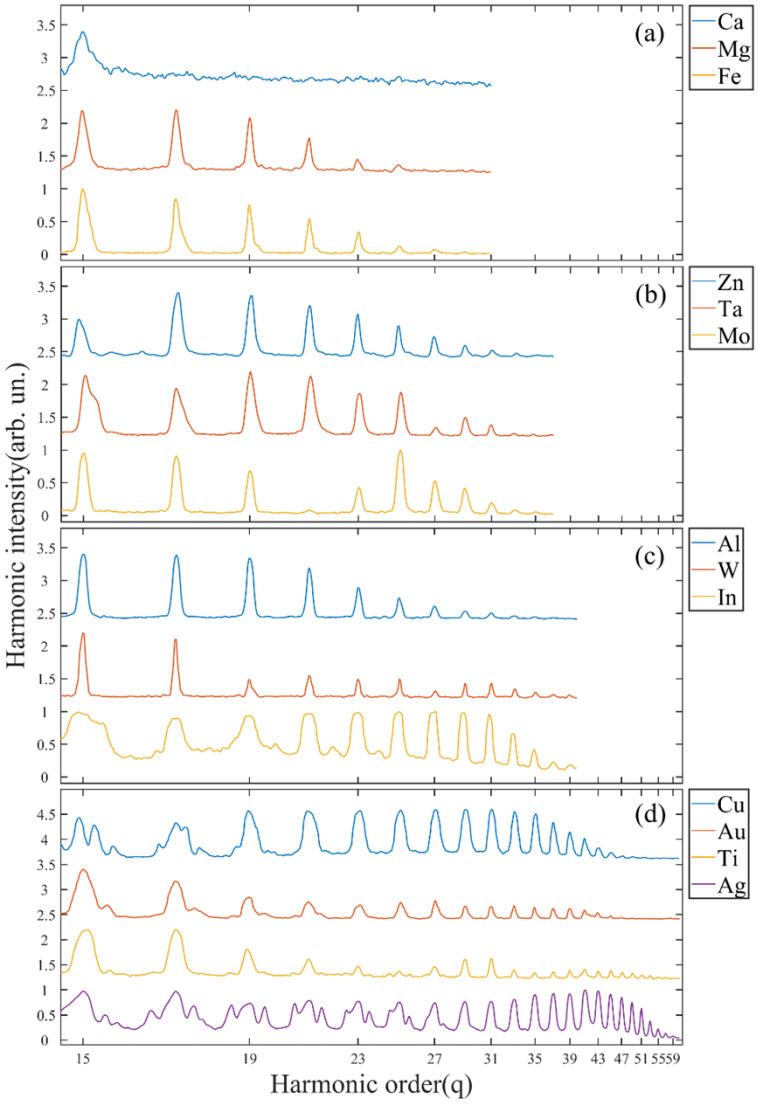

Fig. 2. High-harmonic spectra from the LPP of different metals presented in ascending order by harmonic cutoff: (a) Ca, Mg and Fe; (b) Zn, Ta and Mo; (c) Zn, W and In; (d) Cu, Au, Ti and Ag. Note that the spectra from some targets (e.g. In, Ag) have significantly boarder harmonic peaks are just due to significant saturation of the detector.

Optics EXPRESS

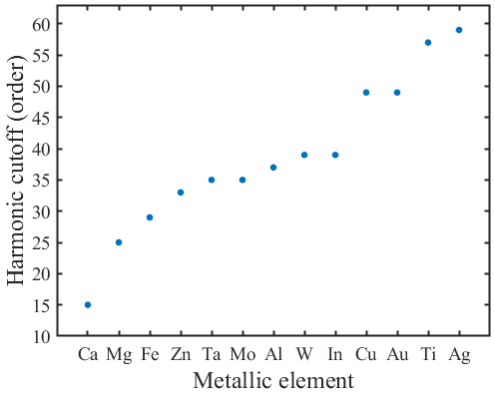

Fig. 3. The harmonic cutoff orders of all the spectra presented in Fig. 2.

At first sight, it is not obvious that such variation in cutoffs could be simply attributed to the semiclassical cutoff law $E_{cutoff} = 3.17U_P + I_P$, since the difference in the I_P values of different metal atoms are rather small (see Table 1). However, as we will discuss below, by considering the I_P of ions and taking the effect of ionization saturation into account, it is found that the experimental and the theoretical values for the cutoffs are in reasonable agreement.

Ionization saturation occurs when the DP intensity approaches the so-called saturation intensity I_{sat}, at which the ionization probability reaches one. In that case, a further increase in the DP intensity would not lead to an actual increase in the effective laser intensity for the HHG process. Instead, it would just make the depletion of ground state happens at an earlier time during the rising edge of the DP, and so the target could not effectively experience the intensity (and the corresponding U_P) at the peak of the pulse envelope. Due to the low I_P of metal atoms and singly charged ions, it is anticipated that their I_{sat} are lower than the typically applied intensities in our experiments. Therefore, knowing the values of I_{sat} of the targets is particularly important for obtaining accurate estimates on the effective U_P values in the HHG process. To examine the ionization saturation of different metal atoms and ions, we use the PPT theory to calculate their ionization probabilities due to the DP. Recent studies in strong field ionization showed that PPT theory is applicable in both multiphoton and tunneling regimes not only for noble gases, but also for several kinds of metal atoms [30–32]. The PPT ionization formula and the procedures for calculating ionization probilities are in the Appendix.

Figure 4 shows the calculated probability of ionizing the neutral atoms for nine of the metal species as a function of DP intensity. Throughout the following discussions, I_{sat} is empirically defined as the intensity at which ionization probability reaches 99.9%. The I_{sat} value for each species is indicated by the vertical dashed line in each plot. Clearly, they are all well below 100TW/cm^2. In fact, most of them are lower than the experimental intensities by at least an order of magnitude. Figure 5 shows the predicted cutoffs harmonic orders (rounded to the nearest integer) for each atom species using the cutoff law $E_{cutoff} = 3.17U_P + I_P$, where U_P is calculated using I_{sat} as the laser intensity. The predicted values are all below the 20th order, which are much lower than the experimental results shown in Fig. 3.

The drastic derivation clearly indicates that it is necessary to consider the contributions by the ions rather than the neutral atoms in the LPPs. Figure 6 shows the DP intensity dependence of the ionization probabilities of the singly charged ions for the same nine metal species. All of the I_{sat} values are higher than 400 TW/cm^2, except for Ca^+ and Mg^+. The blue squares in Fig. 7 are the predicted cutoff harmonic orders (rounded to the nearest integer) using the same cutoff law as in Fig. 6 but here the I_{sat} values for the ions are used as the laser intensities. The red circles show the experimental cutoffs. Overall, good agreements between theory and experiments are

Optics EXPRESS

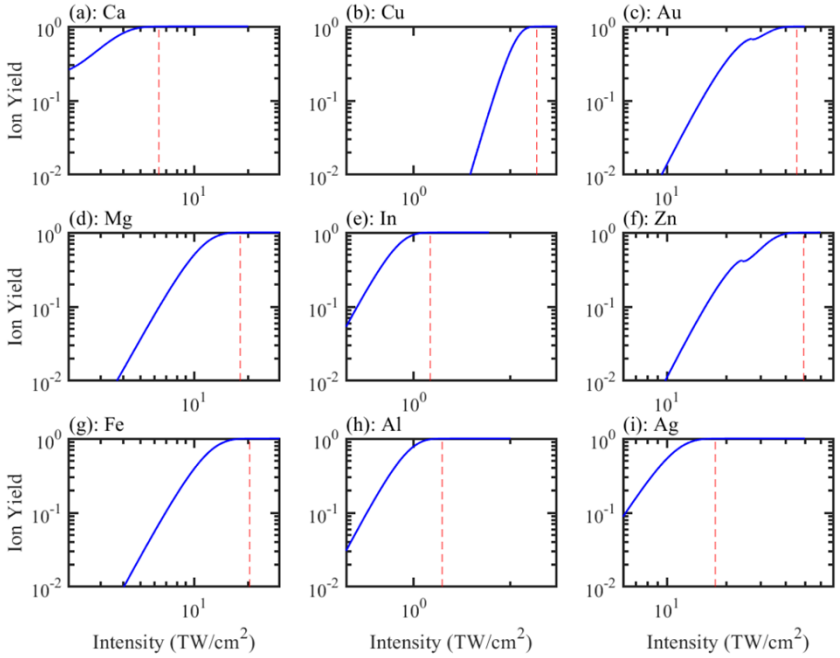

Fig. 4. Calculated ionization probabilities as a function of the DP intensity for the atoms of (a) Ca, (b) Cu, (c) Au, (d) Mg, (e) In, (f) Zn, (g) Fe, (h) Al, and (i) Ag. The saturation intensities Isat are labeled by the red dash lines.

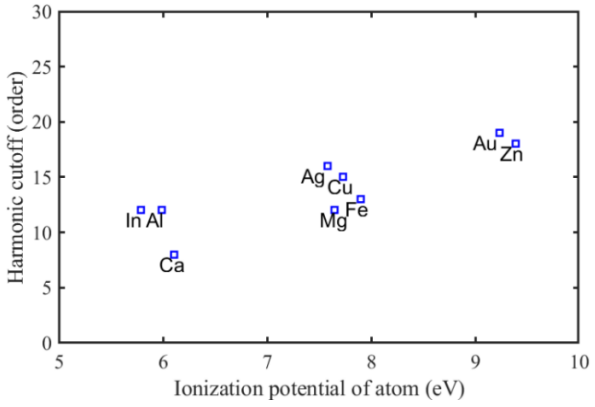

Fig. 5. Predicted cutoffs of different metal targets by the semiclassical cutoff law assuming that the harmonics are generated by neutral atoms and the DP intensities are given by the I_{sat} values found in Fig. 4.

Optics EXPRESS

found. Note that if I_{sat} is empirically defined as the intensity at which ionization probability reaches 99.5% instead of 99.9%, the predicted cutoff order will just slightly decrerase by 1 for most targets in Fig. 7.

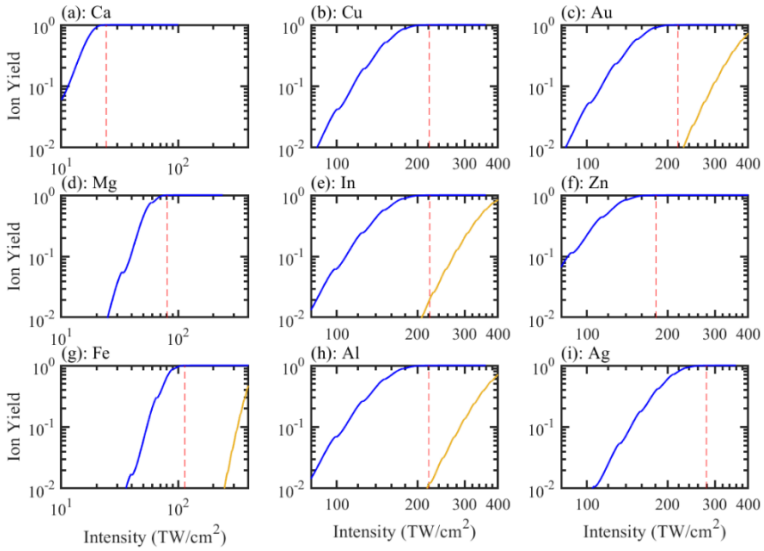

Fig. 6. Calculated ionization probabilities as a function of the DP intensity for the singly charged ions (blue) and doubly charged ions (yellow) of (a) Ca, (b) Cu, (c) Au, (d) Mg, (e) In, (f) Zn, (g) Fe, (h) Al, and (i) Ag. The I_{sat} for the singly charged ions are labeled by the red dash lines.

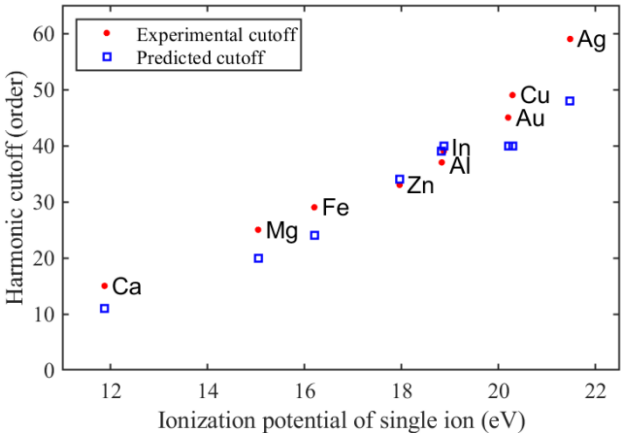

Fig. 7. Experimental harmonic cutoffs (red) vs predicted harmonic cutoffs (blue) by the semiclassical cutoff law for the nine different targets considered in Fig. 6. The predictions are based on the assumptions that the harmonics are generated by singly charged ions and the DP intensities are given by the I_{sat} values found in Fig. 6.

In principle, if the DP intensity is sufficiently high, the ionization of the doubly charged ions should not be overlooked as well. The yellow lines in Fig. 6 show the calculated ionization probabilities of doubly charged ions. Only the results for Fe^{2+}, In^{2+}, Al^{2+} and Au^{2+} are presented. All the others only have very low probabilities (<<1%) and so we believe that the contribution by

Optics EXPRESS

the doubly charged ions in these cases can be neglected. However, the ionization probabilities of the four mentioned species are quite significant (in the order of 10%) when the DP intensity is at 300–400 TW/cm^2. Nevertheless, if the observed cutoffs in these species are indeed contributed by double ions, the predicted cutoffs would be about the 67th order assuming the DP intensity is 400 TW/cm^2. That is significantly higher than the observed values. The maximum DP intensity that our setup could provide is about 700 TW/cm^2, and the harmonic cutoff orders with that intensity are still the same as the results in Fig. 7. It is noteworthy that a previous HHG study on the LPPs of Al [23] also indicated that the harmonic cutoff is about the same even if the DP intensity is even increased to 1000 TW/cm^2. Such limiting behavior might be originated by the free electron-induced self-defocusing effect of the DP propagating in the plasma [33,34]. This effect is more severe for higher DP intensity. Because of this process, the actual DP intensity would be lower than the nominal value.

The I_{sat} of the doubly charged ions of the nine metal species discussed above are relatively high. In the following, we examine the other four species, Mo, Ta, Ti and W. Due to the relatively low I_P of their doubly charged ions, the corresponding I_{sat} are significantly lower (<400 TW/cm^2). As presented in Fig. 8, the blue and yellow lines respectively show the ionization probability of singly and doubly charged ions as a function of DP intensity. The red and the green dashed lines indicate the I_{sat} of the two charge states, respectively. As shown, the I_{sat} for all four doubly charged ions are below 400 TW/cm^2. We use the cutoff law to calculate I_{sat} values of singly and doubly charged ions to compute the predicted cutoffs. The results are shown by the blue and yellow squares in Fig. 9, respectively. The experimental cutoffs are significantly higher than the predicted cutoffs from the singly charged ions. In particular, for Ta, W and Ti, the experimental cutoffs are quite close to the predicted cutoffs from the doubly charged ions.

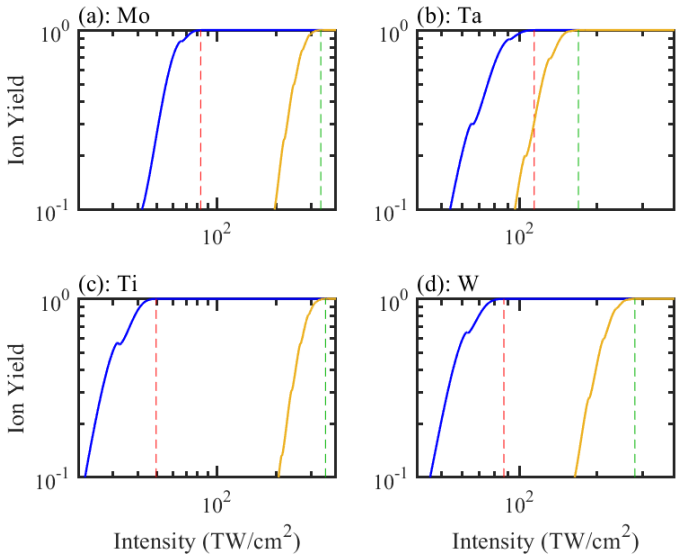

Fig. 8. Calculated ionization probabilities as a function of the DP intensity for the singly charged ions (blue) and doubly charged ions (yellow) of (a) Mo, (b) Ta, (c) Ti, and (d) W. The Isat for the singly and doubly charged ions are labelled by the red and green dash lines, respectively.

Overall, the results so far seem to suggest that the difference in cutoffs between the LPPs from various metal species could be qualitatively understood simply by considering the difference in I_P. Nevertheless, we try to investigate whether there is any alternative reason that might cause the cutoff difference. In principle, if the generation medium itself is strongly absorptive

Optics EXPRESS

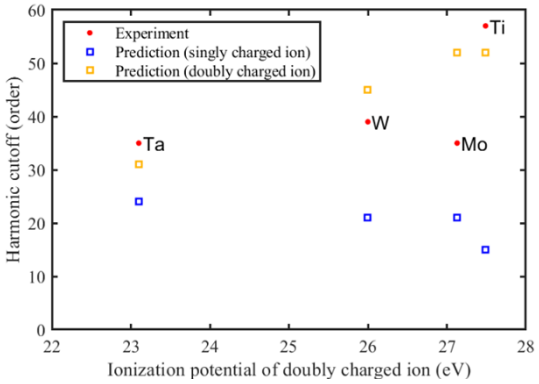

Fig. 9. Experimental harmonic cutoffs (red) vs predicted harmonic cutoffs (blue and yellow) by the semiclassical cutoff law for the four different targets considered in Fig. 8. Blue: predicted values based on the assumptions that the harmonics are generated by singly charged ions and the DP intensities are given by the I_{sat} values indicated by the red lines in Fig. 8. Yellow: predicted values based on the assumptions that the harmonics are generated by doubly charged ions and the DP intensities are given by the I_{sat} values indicated by the green lines in Fig. 8.

in the frequency range near the cutoff region of the harmonic spectrum, the re-absorption of the generated harmonics could lead to a limitation for the harmonic energy [35]. To examine the significance of such absorption effect in LPPs, especially for the species which give low harmonic cutoff, we perform the following test with dual metal targets.

As shown in Fig. 10(b)-(d), two metal targets, Mg and Ag, are put next to each other. Mg is chosen because it is one of the metal species that gives low harmonic cutoff. The harmonics from Ag plasma is used as a tool to test whether the Mg plasma is strongly absorptive. Two beams of HPs are prepared such one beam is aimed at the surface of each target. If both beams are allowed to reach the targets, two plasma plumes are generated from Mg and Ag simultaneously, as shown in Fig. 10(d). If one of the HP beams is disabled, then only one plasma plume is generated either from Mg or Ag, as shown in Fig. 10(b) and (c). Same as the previous experiments, the HHG process is driven by a DP which arrives 50 ns later. After the creation of the plasma plume(s). The harmonic spectrum obtained from Mg and Ag alone are shown by the black and blue lines in Fig. 10(a), respectively. As discussed previously, the harmonic spectrum from Mg plasma has a much lower cutoff than that of Ag plasma.

In the arrangement of Fig. 10(d) with two plasma plumes, the DP first interacts with the Ag plasma and so the generated harmonics will pass through the Mg plasma before being detected. If the Mg plasma is strongly absorptive, then the detected harmonic spectrum should be attenuated compared with the case of Fig. 10(c) in which only Ag plasma is present. However, we find that the spectrum is essentially unaffected by its propagation through the Mg plasma, as shown by the red line in (a). This simple test clearly show that absorption is not a fundamental reason for the low harmonic cutoff in Mg plasma.

Optics EXPRESS

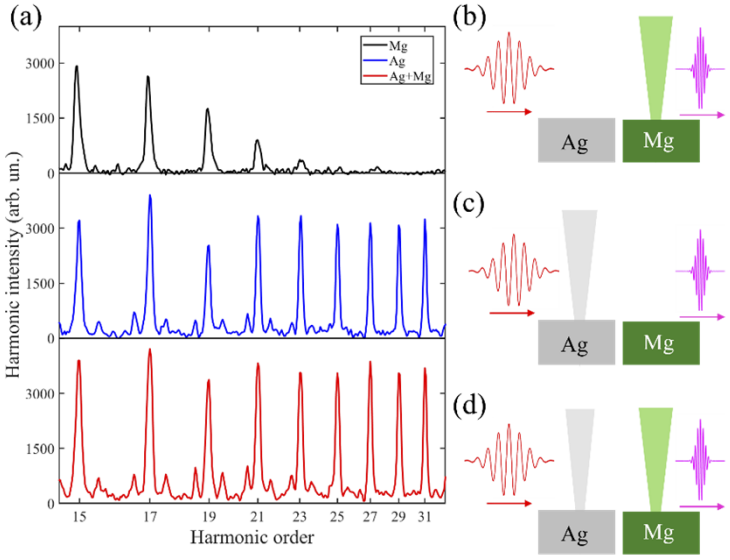

Fig. 10. The experiments about the Mg plasma plume's absorption. (a) Harmonic spectra generated by Mg, Ag, Ag + Mg plasma plume. (b), (c) and (d) are the schematic diagram about the DP interacting with Mg, Ag or Ag + Mg plasma plume.

4. Conclusion

In summary, we have measured and examined the high-harmonic cutoffs from the LPPs of thirteen different metals. PPT theory of strong-field ionization is used to compute the I_{sat} of the atoms and ions of each species. It is found that the observed cutoffs from most of the targets are in reasonable agreement with the predictions of the semi-classical cutoff law if I_{sat} of the singly or doubly charged ions is treated to be the effective driving laser intensity. In addition, the effect of re-absorption of harmonics in LPPs is found to be insignificant and so it should not be the origin of the low harmonic cutoffs observed in some species.

Appendix

The formula of PPT ionization rate is expressed as [28]

$$w_{PPT}(F,\omega) = \sum_{q \geq q_{min}}^{\infty} w_q(F,\omega) \tag{1}$$

where ω and F are the frequency and amplitude of the laser field, respectively. The partial rate w_q is the q-photon above threshold ionization rate. $q_{min} \equiv (I_p + U_p)/\omega$, which is the minimum number of photons required to reach the effective ionization threshold $I_p + U_p$. The full cycle-averaged PPT formula is

$$\begin{aligned} w_{PPT}(F,\omega) = c^2_{n^*l^*} f(l,m) I_p \left(\frac{2}{Fn^{*3}}\right)^{2n^*-|m|-1} \sqrt{\frac{3Fn^{*3}}{\pi}} \times \\ (1+\gamma^2)^{|m|/2+3/4} A_m(\omega,\gamma) \exp\left[-\frac{2(2I_p)^{3/2}}{3F} g(\gamma)\right] \end{aligned} \tag{2}$$

where

$$g(\gamma) = \frac{3}{2\gamma}\left[\left(1+\frac{1}{2\gamma^2}\right)\sinh^{-1}\gamma - \frac{\sqrt{1+\gamma^2}}{2\gamma}\right],$$

Optics EXPRESS

$$A_m(F,\omega) = \frac{4\gamma^2}{\sqrt{3\pi}|m|!(1+\gamma^2)} \sum_{q\geq q_{min}}^{\infty} e^{-\alpha(\gamma)(q-\nu)} w_m\left(\sqrt{\frac{2\gamma}{\sqrt{1+\gamma^2}}}(q-q_{min})\right),$$

$$w_m(x) = \frac{x^{2|m|+1}}{2}\int_0^1 \frac{e^{-x^2 t}t^{|m|}}{\sqrt{1-t}}dt$$

$$\alpha(\gamma) = 2\left(\sinh^{-1}\gamma - \frac{\gamma}{\sqrt{1+\gamma^2}}\right),$$

$$\nu = \frac{I_p}{\omega}\left(1+\frac{1}{2\gamma^2}\right),$$

$$c^2_{n^*l^*} = \frac{2^{2n^*}}{n^*\Gamma(n^*+l^*+1)\Gamma(n^*-l^*)}, \text{and}$$

$$f(l,m) = \frac{(2l+1)(l+|m|)!}{2^{|m|}(|m|)!(l-|m|)!}$$

In the equations above, $\Gamma(x)$ is the gamma function, $n^* = 1/\sqrt{2I_p}$ is the effective quantum number, $l^* = n^* - 1$ is the effective orbital quantum number, and l and m are orbital and magnetic quantum numbers, respectively. The quantization axis is given by the laser polarization direction.

Using the formula for ionization rate, ionization probabililty of an atom (or ion) by a laser pulse is given by

$$P = 1 - \exp\left[-\int_{-\infty}^{+\infty} w(F_0(t))dt\right], \tag{3}$$

where $F_0(t)$ is the pulse envelope function. In our calculations, $F_0(t)$ is a sine-squared function. The pulse duration is defined by the full-width-at-maximum of $[F_0(t)]^2$.

For each atomic (or ionic) species, the ionization probability is calculated as a function of laser intensity, as shown in Fig. 4, 6 and 8.

Funding. National Natural Science Foundation of China (12004380, 62121005); Innovation Grant of Changchun Institute of Optics, Fine Mechanics and Physics (CIOMP); Jilin Provincial Science & Technology Development Project (YDZJ202102CXJD002).

Disclosures. The authors declare no competing financial interest.

Data availability. Data underlying the results presented in this paper are not publicly available at this time but may be obtained from the authors upon reasonable request.

References

1. H. Kapteyn, O. Cohen, I. Christov, and M. Murnane, "Harnessing Attosecond Science in the Quest for Coherent X-rays," Science **317**(5839), 775–778 (2007).
2. F. Krausz and M. Ivanov, "Attosecond physics," Rev. Mod. Phys. **81**(1), 163–234 (2009).
3. R. A. Ganeev, "Generation of harmonics of laser radiation in plasmas," Laser Phys. Lett. **9**(3), 175–194 (2012).
4. M. A. Fareed, V. V. Strelkov, M. Singh, N. Thire, S. Mondal, B. E. Schmidt, F. Legare, and T. Ozaki, "Harmonic Generation from Neutral Manganese Atoms in the Vicinity of the Giant Autoionization Resonance," Phys. Rev. Lett. **121**(2), 023201 (2018).
5. M. Singh, M. A. Fareed, V. Strelkov, A. N. Grum-Grzhimailo, A. Magunov, A. Laramée, F. Légaré, and T. Ozaki, "Intense quasi-monochromatic resonant harmonic generation in the multiphoton ionization regime," Optica **8**(8), 1122–1125 (2021).
6. R. A. Ganeev, M. Suzuki, M. Baba, H. Kuroda, and T. Ozaki, "Strong resonance enhancement of a single harmonic generated in the extreme ultraviolet range," Opt. Lett. **31**(11), 1699–1701 (2006).
7. M. Suzuki, M. Baba, R. Ganeev, H. Kuroda, and T. Ozaki, "Anomalous enhancement of a single high-order harmonic by using a laser-ablation tin plume at 47 nm," Opt. Lett. **31**(22), 3306–3308 (2006).
8. N. Rosenthal and G. Marcus, "Discriminating between the Role of Phase Matching and that of the Single-Atom Response in Resonance Plasma-Plume High-Order Harmonic Generation," Phys. Rev. Lett. **115**(13), 133901 (2015).
9. M. Suzuki, M. Baba, H. Kuroda, R. A. Ganeev, and T. Ozaki, "Intense exact resonance enhancement of single-high-harmonic from an antimony ion by using Ti : Sapphire laser at 37 nm," Opt. Express **15**(3), 1161–1166 (2007).

Optics EXPRESS

10. V. Strelkov, "Role of Autoionizing State in Resonant High-Order Harmonic Generation and Attosecond Pulse Production," Phys. Rev. Lett. **104**(12), 123901 (2010).
11. M. A. Fareed, V. V. Strelkov, N. Thiré, S. Mondal, B. E. Schmidt, F. Légaré, and T. Ozaki, "High-order harmonic generation from the dressed autoionizing states," Nat. Commun. **8**(1), 16061 (2017).
12. G. S. J. Armstrong, M. A. Khokhlova, M. Labeye, A. S. Maxwell, E. Pisanty, and M. Ruberti, "Dialogue on analytical and ab initio methods in attoscience," Eur. Phys. J. D **75**(7), 209 (2021).
13. M. A. Khokhlova, M. Y. Emelin, M. Y. Ryabikin, and V. V. Strelkov, "Polarization control of quasimonochromatic XUV light produced via resonant high-order harmonic generation," Phys. Rev. A **103**(4), 043114 (2021).
14. M. Lewenstein, P. Balcou, M. Y. Ivanov, A. L'Huillier, and P. B. Corkum, "Theory of high-harmonic generation by low-frequency laser fields," Phys. Rev. A **49**(3), 2117–2132 (1994).
15. Z. Chang, A. Rundquist, H. Wang, M. M. Murnane, and H. C. Kapteyn, "Generation of Coherent Soft X Rays at 2.7 nm Using High Harmonics," Phys. Rev. Lett. **79**(16), 2967–2970 (1997).
16. E. J. Takahashi, T. Kanai, Y. Nabekawa, and K. Midorikawa, "10mJ class femtosecond optical parametric amplifier for generating soft x-ray harmonics," Appl. Phys. Lett. **93**(4), 041111 (2008).
17. M.-C. Chen, P. C. Arpin, T. Popmintchev, M. Gerrity, B. Zhang, M. H. Seaberg, D. Popmintchev, M. M. Murnane, and H. C. Kapteyn, "Bright, coherent, ultrafast soft X-ray harmonics spanning the water window from a tabletop light source," Phys. Rev. Lett. **105**(17), 173901 (2010).
18. G. Cirmi, C.-J. Lai, E. Granados, S.-W. Huang, A. Sell, K.-H. Hong, J. Moses, P. Keathley, and F. X. Kärtner, "Cut-off scaling of high-harmonic generation driven by a femtosecond visible optical parametric amplifier," J. Phys. B: At., Mol. Opt. Phys. **45**(20), 205601 (2012).
19. T. Popmintchev, M.-C. Chen, D. Popmintchev, P. Arpin, S. Brown, S. Ališauskas, G. Andriukaitis, T. Balčiunas, O. D. Mücke, A. Pugzlys, A. Baltuška, B. Shim, S. E. Schrauth, A. Gaeta, C. Hernández-García, L. Plaja, A. Becker, A. Jaron-Becker, M. M. Murnane, and H. C. Kapteyn, "Bright Coherent Ultrahigh Harmonics in the keV X-ray Regime from Mid-Infrared Femtosecond Lasers," Science **336**(6086), 1287–1291 (2012).
20. R. A. Ganeev and H. Kuroda, "Frequency conversion of femtosecond radiation in magnesium plasma," Opt. Commun. **256**(4-6), 242–247 (2005).
21. R. A. Ganeev and H. Kuroda, "High-Order Harmonics Generation in Atomic and Molecular Zinc Plasmas," Photonics **8**(2), 29 (2021).
22. V. V. Kim, G. S. Boltaev, M. Iqbal, N. A. Abbasi, H. Al-Harmi, I. S. Wahyutama, T. Sato, K. L. Ishikawa, R. A. Ganeev, and A. S. Alnaser, "Resonance enhancement of harmonics in the vicinity of 32 nm spectral range during propagation of femtosecond pulses through the molybdenum plasma," Journal of Physics B-Atomic Molecular and Optical Physics **53**(2020).
23. R. A. Ganeev, M. Suzuki, M. Baba, and H. Kuroda, "33rd harmonic generation from aluminium plasma," J. Mod. Opt. **53**(10), 1451–1458 (2006).
24. M. Woestmann, P. V. Redkin, J. Zheng, H. Witte, R. A. Ganeev, and H. Zacharias, "High-order harmonic generation in plasmas from nanoparticle and mixed metal targets at 1-kHz repetition rate," Appl. Phys. B **120**(1), 17–24 (2015).
25. R. A. Ganeev, M. Suzuki, M. Baba, M. Ichihara, and H. Kuroda, "Low- and high-order nonlinear optical properties of Au, Pt, Pd, and Ru nanoparticles," J. Appl. Phys. **103**(6), 063102 (2008).
26. M. Suzuki, R. A. Ganeev, L. B. E. Bom, M. Baba, T. Ozaki, and H. Kuroda, "Extension of cutoff in high harmonic by using doubly charged ions in a laser-ablation plume," J. Opt. Soc. Am. B **24**(11), 2847–2852 (2007).
27. R. A. Ganeev, M. Baba, M. Suzuki, and H. Kuroda, "High-order harmonic generation from silver plasma," Phys. Lett. A **339**(1-2), 103–109 (2005).
28. A. M. Perelomov, V. S. Popov, and M. V. Terent'ev, "Ionization of Atoms in an Alternating Electric Field," Soviet Journal of Experimental and Theoretical Physics **23**, 924 (1966).
29. R. A. Ganeev, L. B. E. Bom, T. Ozaki, and P. V. Redkin, "Maximizing the yield and cutoff of high-order harmonic generation from plasma plume," J. Opt. Soc. Am. B **24**(11), 2770–2778 (2007).
30. Y. H. Lai, J. Xu, U. B. Szafruga, B. K. Talbert, X. Gong, K. Zhang, H. Fuest, M. F. Kling, C. I. Blaga, P. Agostini, and L. F. DiMauro, "Experimental investigation of strong-field-ionization theories for laser fields from visible to midinfrared frequencies," Phys. Rev. A **96**(6), 063417 (2017).
31. H. Kang, S. Chen, Z. Lin, W. Chu, J. Yao, W. Quan, J. Chen, X. Liu, Y. Cheng, and Z. Xu, "Comparative study of strong-field ionization of alkaline-earth-metal atoms," Phys. Rev. A **101**(5), 053433 (2020).
32. Y. H. Lai, X. Wang, Y. Li, X. Gong, B. K. Talbert, C. I. Blaga, P. Agostini, and L. F. DiMauro, "Experimental test of recollision effects in double ionization of magnesium by near-infrared circularly polarized fields," Phys. Rev. A **101**(1), 013405 (2020).
33. C.-J. Lai and F. X. Kärtner, "The influence of plasma defocusing in high harmonic generation," Opt. Express **19**(23), 22377–22387 (2011).
34. H.-W. Sun, P.-C. Huang, Y.-H. Tzeng, J.-T. Huang, C. D. Lin, C. Jin, and M.-C. Chen, "Extended phase matching of high harmonic generation by plasma-induced defocusing," Optica **4**(8), 976–981 (2017).
35. T. T. Luu, Z. Yin, A. Jain, T. Gaumnitz, Y. Pertot, J. Ma, and H. J. Wörner, "Extreme–ultraviolet high–harmonic generation in liquids," Nat Commun **9**(1), 3723 (2018).